0026-895X/06/6905-1579–1587$20.00
MOLECULAR PHARMACOLOGY
Copyright © 2006 The American Society for Pharmacology and Experimental Therapeutics
*Mol Pharmacol* 69:1579–1587, 2006

Vol. 69, No. 5
20669/3108115
*Printed in U.S.A.*





# Celecoxib Inhibits Interleukin-12 $\alpha\beta$ and $\beta_2$ Folding and Secretion by a Novel COX2-Independent Mechanism Involving Chaperones of the Endoplasmic Reticulum

Iraide Alloza, Andy Baxter, Qian Chen, Rune Matthiesen, and Koen Vandenbroeck

*Applied Genomics Research Group, School of Pharmacy, McClay Research Center for Pharmaceutical Sciences, Queen's University Belfast, Belfast, United Kingdom (I.A., K.V.); Arakis Ltd., Saffron Walden, Essex, United Kingdom (A.B.); Department of Immunology, Queen's University of Belfast, Belfast, United Kingdom (Q.C.); and Bioinformatics Group, CIC bioGUNE, Bilbao, Spain (R.M.)*

Received November 8, 2005; accepted February 7, 2006

## ABSTRACT

Celecoxib (CE) is a nonsteroidal anti-inflammatory drug (NSAID) that is a specific inhibitor of cyclooxygenase 2 (COX2). It is indicated for a variety of chronic inflammatory conditions, including rheumatoid arthritis. Over the last few years, adverse cardiovascular effects and increased risk for heart attacks have been associated with this drug. In addition, evidence is emerging for COX2-independent molecular targets. CE has been shown to induce apoptosis in various cancer cells lines through a COX2-independent mechanism that seems to involve inactivation of protein kinase Akt and inhibition of endoplasmic reticulum (ER) $Ca^{2+}$ ATPase. In this study, we show that both CE and an analog devoid of COX2 inhibitory activity [1-(4-sulfamoyl phenyl)-3-trifluoromethyl-5-(4-trifluoromethylphenyl)pyrazole, CEA] inhibit the secretion of the dimeric interleukin-12 (IL-12) $\alpha\beta$ and $\beta_2$ forms with identical $IC_{50}$ values of 20 and 30 $\mu$M, respectively, whereas no such effect was seen with rofecoxib. Reverse transcription-polymerase chain reaction analysis showed that this inhibition was not due to a blockage of transcription of the $\alpha$- and $\beta$-chain expression cassettes. Secretion of the $\beta$ monomer form was less strongly inhibited, suggestive for a mechanism primarily targeting dimer assembly in the ER. Analysis of intracellular fractions revealed that both CE and CEA increased the association of IL-12 with calreticulin, an endoplasmic reticulum-resident chaperone involved in the retention of misfolded cargo proteins while blocking interaction with ERp44. Our findings reveal a previously undescribed effect of celecoxib on oligomer protein folding and assembly in the endoplasmic reticulum and ensuing secretion and suggest that celecoxib-driven alteration of the secretome may be involved in some of its clinical side effects.

Interleukin-12 (IL-12) is a proinflammatory cytokine involved in the initiation and control of cell-mediated immunity. The cytokine displays a heterodimeric structure composed of two disulfide-linked subunits [i.e., a p35 ($\alpha$-chain) and a p40 ($\beta$-chain) subunit] (Brombacher et al., 2003). p40 can also form disulfide-linked homodimers, named $\beta_2$ or p80. $\beta_2$ Homodimers were originally described as antagonists of IL-12. However, more recent studies have ascribed chemotactic properties to the $\beta_2$ homodimer (Ha et al., 1999). $\beta_2$ Homodimers were also found to play a disease-promoting role in airway inflammation (Walter et al., 2001).

There is ample evidence of a crucial role for IL-12 in the pathogenesis of TH1-mediated autoimmune diseases, including multiple sclerosis, rheumatoid arthritis, and inflammatory bowel disease (Trembleau et al., 1995). Thus, pharmacological control of IL-12 production is a possible strategy in the development of future treatments for such diseases (Vandenbroeck et al., 2004).

Nonsteroidal anti-inflammatory drugs (NSAIDs) are indicated for the treatment of a variety of chronic inflammatory diseases and act by inhibiting prostaglandin H synthase (also known as cyclooxygenase, COX). There are two forms of this enzyme, COX1 and COX2. COX1 is expressed constitutively

This work was supported by the Northern Ireland R&D Office, grant RRG11.5.

Article, publication date, and citation information can be found at http://molpharm.aspetjournals.org.

doi:10.1124/mol.105.020669.

**ABBREVIATIONS:** IL-12, interleukin-12; NSAID, nonsteroidal anti-inflammatory drug; CE, celecoxib; CEA, 1-(4-sulfamoyl phenyl)-3-trifluoromethyl-5-(4-trifluoromethylphenyl)pyrazole; COX2, cyclooxygenase 2; ER, endoplasmic reticulum; HEK, human embryonic kidney cells; MTT, 3-[4,5-dimethylthiazol-2-yl]-2,5-diphenyltetrazolim bromide; $Ni^{2+}$-NTA, nickel-nitrilotriacetic acid; HA, hemagglutinin; wt, wild type; GADPH, glyceraldehyde-3 phosphate dehydrogenase; CRT, calreticulin; TG, thapsigargin; TH, thyroglobulin; NEM, *N*-ethylmaleimide; DSP, dithiobis(succinimidylpropionate); PAGE, polyacrylamide gel electrophoresis; RT-PCR, reverse transcription-polymerase chain reaction; HBSS, Hanks' balanced salt solution; FAM, 5-carboxyfluorescein; AM, acetoxymethyl ester.

in most tissues, whereas COX2 is inducible and localized at the site of inflammation and up-regulated in cancer (Vane et al., 1994; Subbaramaiah et al., 1996). Inhibition of COX1 by nonspecific NSAIDs can cause gastric injury. To avoid this side effect, selective COX2 inhibitors have been developed (i.e., celecoxib, rofecoxib, and valdecoxib) for the treatment of inflammatory diseases (DeWitt, 1999). Recent studies have demonstrated the utility of COX2 inhibitors as chemopreventive anticancer agents as well (Sheng et al., 1997; Prescott and Fitzpatrick, 2000).

Although celecoxib (CE) was originally designed as a COX2 inhibitor, there is increasing evidence that this compound also can exert COX2-independent effects (Tegeder et al., 2001). The anticancer activity of CE has been associated with its ability to induce apoptosis in cancer cells. CE has been shown to provoke a cell-cycle arrest and a decrease of cell survival in colon cancer cell lines, whether or not they produce COX2 (Grosch et al., 2001). These authors also showed that this effect is associated with a decrease in the production of cyclins and an increase in the expression of the cell cycle inhibitory proteins $p21^{Waf1}$ and $p27^{Kip1}$ with an $EC_{50}$ value between 50 and 100 $\mu$M.

CE was found also to inhibit the protein kinase B/Akt pathway in prostate cancer cells (Hsu et al., 2000; Kulp et al., 2004). Patel et al. (2005) showed that CE, but not rofecoxib, inhibits cell growth in human prostate cell lines that do not produce COX2. Kulp et al. (2004) used CE and a COX2 inactive analog to study their effect on prostate cancer cells. They found that the mechanism by which these drugs exert their anticancer effects is through the 3-phosphoinositide-dependent protein kinase-1/Akt signaling pathway. It is known that 3-phosphoinositide-dependent protein kinase-1/Akt signaling plays a significant role in cancer cell growth and survival (Vivanco and Sawyers, 2002).

CE induces an increase of intracellular calcium in prostate cancer cells and osteoblasts that is not observed with other NSAIDs (Johnson et al., 2002; Wang et al., 2004). This effect is caused by the inhibition of endoplasmic reticulum (ER) $Ca^{2+}$ ATPase, and is dose- and time-dependent (Johnson et al., 2002; Wang et al., 2004). CE is also capable of inhibiting adenyl cyclase. This inhibition is COX2-independent and causes platelet aggregation because of a decrease of cAMP (Saini et al., 2003). All together, these facts show the complexity and diversity of COX2-independent actions of CE.

In the present study, we characterized a novel mechanism by which celecoxib (4-[5-(4-methylphenyl)-3-(trifluoromethyl)-1*H*-pyrazol-1-yl] benzenesulfonamide) (CE) and the COX2-inactive analog 1-(4-sulfamoyl phenyl)-3-trifluoromethyl-5-(4-trifluoromethylphenyl)pyrazole (CEA) block the secretion of the dimeric forms of interleukin-12. Our data reveal a post-transcriptional effect on IL-12 folding in the ER that is possibly $Ca^{2+}$-dependent and involves the ER-resident chaperones calreticulin and ERp44.

## Materials and Methods

**Chemical Synthesis of CEA.** The COX2-inactive analog CEA was synthesized by Onyx Scientific (Sunderland, UK). The procedure used to synthesize CEA was similar to that reported by Penning et al. (1997).

**Cell Culture Conditions and Inhibitors.** 3H10-HEK EcR-293 cells (Invitrogen, Paisley, UK) were cultivated in Dulbecco's modified Eagle's medium (Invitrogen) supplemented with 10% of fetal bovine serum, 2 mM L-glutamine, 400 $\mu$g/ml zeocin, and 600 $\mu$g/ml G418. Cells were maintained in a $CO_2$ incubator at 37°C (5% $CO_2$). Cells were treated with various concentrations (see *Results*) of CE (Hefei Scenery Chemicals, Anhui, China) or celecoxib analog (CEA; Arakis, Saffron Walden, UK) 2 h before induction with ponasterone A (Invitrogen). Rofecoxib was obtained from Hefei Scenery Chemicals, and the other NSAIDs were from Sigma-Aldrich (Poole, Dorset, UK).

**Transient Transfection of 3H10-HEK Cells with $\alpha$-Chain Construct.** Development of the $\beta$-chain-producing cell line (3H10-HEK) has been described before (Alloza et al., 2004). This cell line produces a mixture of both $\beta_2$ homodimers and $\beta$ monomers (Alloza et al., 2004) and can be converted into a cell line producing IL-12 $\alpha\beta$ heterodimers by transient transfection with the vector pIND(SP1)-p35 that contains a cDNA coding for the $\alpha$-chain. To this purpose, 3H10-HEK cells were plated the day before transfection at a confluence of $10^5$ cells/well. Vector DNA (1 $\mu$g) containing the $\alpha$-chain coding sequence [pIND(SP1)-p35] was used to transform 3H10-HEK cells using 3 $\mu$l of reagent FuGENE-6 (Roche Diagnostics, Basel, Switzerland). Cells were allowed to recover during 24 h before induction with ponasterone A. Both the $\alpha$- and $\beta$-chains are produced and secreted into culture medium as C-terminally hexahistidine-tagged proteins that can be purified on $Ni^{2+}$-nickel-nitrilo-triacetic acid (NTA) agarose (Alloza et al., 2004).

**Cytotoxicity Tests.** A culture of $10^5$ cells/well was prepared in 96-well plates the day before the experiment. Cells were treated with a concentration series of drugs (0.01–400 $\mu$M CE or CEA; 1–100 $\mu$M ibuprofen, indomethacin, or rofecoxib; or 1–50 $\mu$M naproxen) and subsequently induced with ponasterone A. After 24 h of induction, 10 $\mu$g/ml 3-[4,5-dimethylthiazol-2-yl]-2,5-diphenyltetrazolim bromide (MTT) reagent was added to the cells. After 2 h of incubation, the formed formazan crystals were dissolved in 200 $\mu$l of dimethyl sulfoxide. The obtained solution was measured in a spectrophotometer at 550 nm. As a positive control, untreated cells were used.

**Purification of Hexahistidine-Tagged $\beta_2$ and $\alpha\beta$ Forms.** 3H10-HEK cells and transfected 3H10-HEK cells were treated with CE or CEA for 24 h. Purification of intracellular IL-12 folding complexes was performed using $Ni^{2+}$-NTA affinity chromatography (QIAGEN, West Sussex, UK), as described before (Alloza et al., 2004). Cultured medium was collected and mixed with a equal amount of 2× binding buffer [100 mM $NaH_2PO_4$, 600 mM NaCl, 40 mM imidazole, 2% of generic protease inhibitors, 20 mM *N*-ethylmaleimide (NEM), pH 8] together with 60 $\mu$l of prewashed $Ni^{2+}$-NTA agarose. NEM was added to block oxidative formation of disulfide bonds by alkylation of free sulfhydryl groups. 3H10-HEK cells were lysed in lysis buffer (50 mM $NaH_2PO_4$, 300 mM NaCl, 20 mM imidazole, 0.5% Triton X-100, 1% of protease inhibitors, and 10 mM NEM, pH 8) on ice for 30 min. After 15 min of centrifugation at 15,000 rpm, the supernatants were mixed with 10 $\mu$l of prewashed $Ni^{2+}$-NTA agarose. Both cultured medium and supernatant solutions were incubated for 1 h at 4°C on a rotating wheel. Agarose beads were washed with 1× binding buffer, pH 6.3, three times followed by elution in 10 $\mu$l of 50 mM EDTA.

**Purification of IL-12-ERp44 Folding Complexes.** 3H10-HEK cells were transfected with 1 $\mu$g of vector DNA containing the influenza A hemagglutinin (HA)-tagged ERp44 wild type (wt), the HA-tagged ERp44 C29S (mutant lacking the C29 cysteine) or the HA-tagged ERp44 ΔRDEL (mutant lacking the RDEL motif) (Anelli et al., 2002, 2003). Subsequently, cells were induced with ponasterone A and treated with CE and CEA. After 24 h, cells were washed with phosphate-buffered saline and lysed in lysis buffer followed by affinity-purification of IL-12-ERp44 complexes on $Ni^{2+}$-NTA agarose, as described above.

**Cross-Linking and Purification of IL-12-Calreticulin Folding Complexes.** 3H10-HEK cells were treated with CEA followed by induction with ponasterone A. After 16 h, cells were washed five times with phosphate-buffered saline. Cells were cross-linked with 10 $\mu$g/ml dithiobis(succinimidylpropionate) (DSP) (Pierce, Cheshire,

UK) or were left un-cross-linked during 30 min at room temperature. DSP was added to stabilize any noncovalent interactions between IL-12 and calreticulin (CRT) against solubilization by detergents used for cell lysis. Reactions were quenched by adding 100 mM Tris-HCl, pH 8.0, and incubated for 15 min at room temperature. Then cells were lysed for 30 min on ice using lysis buffer followed by centrifugation for 15 min at 14,000 rpm. Prewashed $Ni^{2+}$-NTA agarose (20 $\mu$l) was added to cell lysates and incubated at 4°C for 1 h. Agarose beads were washed six times with 1× binding buffer, pH 6.3. Proteins were eluted in 50 mM EDTA in 1× binding buffer, pH 8.0. Eluates were subjected to 4 to 20% reducing SDS-PAGE.

**Western Blot and Immunodetection.** Cultured medium, cell lysates, and affinity-purified eluted fractions were separated on reducing or nonreducing 4 to 20% Tris-glycine gels using the Novex System (Novex, Nuernberg, Germany). To ensure equal loading, protein concentrations were determined by the bicinchoninic acid (Pierce, Rockford, IL) assay before SDS-PAGE, and equal amounts were loaded. After electroblot, membranes were probed with primary antibodies (mouse $\alpha$-p35 antibody, G161-566 and mouse $\alpha$-p40 antibody, C8.6) obtained both from BD Biosciences (Erembodegem-Aalst, Belgium). For detection of ERp44 wild type and mutants, we used the mouse monoclonal HA-antibody (12CA5) from Roche (East Sussex, UK). CRT was detected with the rabbit polyclonal antibody SPA-600 (Stressgen, Victoria, BC, Canada). For detection of albumin secreted from HepG2 cells (cultured in minimal essential medium), the antibody ab19183 was used. Cells were washed four times and grown in fetal bovine serum-free medium for the last 6 h of the 24-h treatment period. The secondary antibodies used were goat anti-mouse or anti-rabbit horseradish peroxidase conjugate antibody obtained from Jackson ImmunoResearch Laboratories (West Grove, PA). Protein bands were detected using the ECL or ECL Plus chemiluminescence detection reagent (Amersham Biosciences, Bucks, UK), and the blots were exposed with an autoradiography film (Kodak, Herts, UK).

**Primers and Probes.** Real-time quantitative polymerase chain reaction (QuantiProbes) primers and probes for IL-12 $\alpha$-chain and $\beta$-chain were purchased from QIAGEN (West Sussex, UK) as functionally validated gene expression assays. A FAM-labeled $\alpha$-chain probe (241047) and a FAM-labeled $\beta$-chain probe (241049) were used. GADPH primers and probe were obtained as predeveloped TaqMan assay reagents from Applied Biosystems (4333764) (Warrington, UK) and were also FAM-labeled.

**Quantification of $\alpha$-Chain and $\beta$-Chain mRNAs by Real-Time RT-PCR.** Cultures of $10^6$ 3H10-HEK cells were grown in the presence of increasing concentrations of CE or CEA. Two hours later, cells were induced with ponasterone A and incubated for a further 22 h. Total RNA was extracted using the Absolutely RNA RT-PCR Miniprep kit (Stratagene, CA). mRNA levels of $\alpha$- and $\beta$-chain were quantified using the RT-PCR Quantitect Gene Expression Assay kit (QIAGEN) on a DNA Engine Opticon 2 (MJ Research, South San Francisco, CA). Real-time RT-PCR was performed by following the supplier's protocol (QIAGEN): 30 min at 50°C, 15 min at 95°C, 45 cycles of 15 s at 94°C, 30 s at 56°C, and 30 s at 76°C. Assay conditions were as follows: 12.5 $\mu$l of 2× QuantiTect Probe RT-PCR Master Mix, 2.5 $\mu$l of 10× Quantiprobe and primer Mix Solution, 0.25 $\mu$l of QuantiTect RT Mix, and 10 to 200 ng of RNA. All of the reactions were replicated in separate tubes for detection of $\alpha$-chain, $\beta$-chain, and GADPH, and the mean values of expression were calculated as below. Control reactions without template were performed to detect nonspecific amplification due to contamination.

**Coloading Cells with $Ca^{2+}$ Indicators (Fluo-3 AM and Fura-Red AM).** 3H10-HEK cells ($10 \times 10^6$ cells) were treated with 50 $\mu$M CE, CEA, or rofecoxib, as indicated above, washed twice with 1× Hanks' balanced salt solution (HBSS) and resuspended in 1 ml of HBSS. Fluo-3 AM (5 $\mu$l/ml) and 10 $\mu$l/ml Fura-Red AM (both from Invitrogen) were added. Cells were then incubated for 30 min at 37°C. During incubation, the cells were shaken a couple of times. To allow complete de-esterification of intracellular AM esters, cells were diluted 1:5 by adding 4 ml of HBSS plus 1% fetal calf serum and incubated for a further 30 min at room temperature. 3H10-HEK cells were then washed three times with HBSS plus 1% fetal calf serum and resuspended in 7 ml of HEPES-buffered saline (137 mM NaCl, 5 mM KCl, 1 mM $Na_2HPO_4$, 5 mM glucose, 1 mM $CaCl_2$, 0.5 mM $MgCl_2$, 1g/l bovine serum albumin, and 10 mM HEPES, pH 7.4). Cells were maintained in darkness until acquisition.

**Flow Cytometry.** Analyses were performed at room temperature on a Cyan flow cytometer (DakoCytomation, Carpinteria, CA). Cells were assayed at rates of 800 cells/s. Summit version 3.3 software was used to collect and plot data. Gating was performed using characteristic forward versus orthogonal light scatter (FSC versus SSC). The fluorescein isothiocyanate filter set was used to detect Fluo-3 signals and the PE-Cy5 filter set was used to detect Fura-Red signals. Both indicators were excited at 488 nm with Fluo-3 emission detected at 515 to 535 nm and Fura-Red emission detected at 665 to 685 nm. Results in the figures were shown as histograms of the fluorescence ratio (Fluo-3/Fura-Red) versus time. The complete run was divided into 450 s. Standard controls included stimulation with the $Ca^{2+}$ ionophore ionomycin (1 $\mu$g/ml).

**Statistical Analysis.** Statistical tests were performed using the statistical R package (http://www.r-project.org/). Test for significant differences between groups was done using analysis of variance and the nonparametric Kruskal-Wallis test. The results from the Kruskal-Wallis test are presented throughout the manuscript because of the relatively few data points (Zar, 1999). Use of analysis of variance tests gave similar results. Multiple comparison tests were performed in the cases in which the Kruskal-Wallis test gave significant differences between groups. The Bonferroni correction was used to adjust for multiple testing. $P < 0.05$ denoted significance in all cases.

## Results

**CE and CEA Block Secretion of $\alpha\beta$ and $\beta_2$ Forms of IL-12.** We investigated the effect of both CE and an analog devoid of COX2 inhibitory activity (CEA) (Penning et al., 1997) on the production of IL-12 (Fig. 1). 3H10-HEK recombinant cells (Alloza et al., 2004) were grown and induced for 24 h with ponasterone A to produce $\beta$ monomers and $\beta_2$ dimers or, alternatively, were first transiently transfected with an $\alpha$-chain expression vector followed by induction to produce IL-12 $\alpha\beta$ heterodimers. Cells were exposed for 24 h to an increasing concentration series of CE or CEA (0–100 $\mu$M). Figure 2, A and B, shows that CE blocks the secretion of

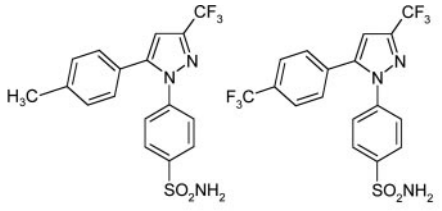


| | CE | CEA |
|---|---|---|
| $IC_{50}$ COX-1 | 15 μM | >100 μM |
| $IC_{50}$ COX-2 | 0.04 μM | 8.2 μM |
| $IC_{50}$ IL-12$\beta_{2secreted}$ | 30 μM | 30 μM |
| $IC_{50}$ IL-12$\alpha\beta_{secreted}$ | 20 μM | 20 μM |

**Fig. 1.** Chemical structures of CE (4-[5-(4-methylphenyl)-3-(trifluoromethyl)-1*H*-pyrazol-1-yl] benzenesulfonamide) and CEA [1-(4-sulfamoylphenyl)-3-trifluoromethyl-5-(4-trifluoromethylphenyl)pyrazole]. The $IC_{50}$ data for inhibition of COX1 and -2 are from Penning et al. (1997). The $IC_{50}$ values for the IL-12 $\alpha\beta$ and $\beta_2$ forms were determined in this study by measuring the effect of CE and CEA on secretion of these cytokines.

$\beta_2$ and $\alpha\beta$ forms, with $IC_{50}$ values of approximately 30 and 20 $\mu$M, respectively. Virtually identical inhibitory curves were seen with CEA (shown for $\beta_2$ in Fig. 2, C and E). CEA did not inhibit secretion of the housekeeping protein albumin (Fig. 2D), and neither did CE (data not shown). Further confirmation that these effects were not due to COX2 inhibition came from an analysis of additional NSAIDs. Rofecoxib is a stronger COX2 inhibitor than CE with an $IC_{50}$ value of 0.018 versus 0.04 $\mu$M (Waskewich et al., 2002), but when tested over a concentration range of 0 to 100 $\mu$M did not show any effect on IL-12 secretion (shown for $\beta_2$ in Figs. 2E and 3). Statistical analysis by means of the Kruskal-Wallis test confirmed the absence of a dose-response effect for rofecoxib on $\beta_2$ secretion, whereas significant dose-response effects were seen for the effects of CE and CEA on secretion of $\beta$ and $\beta_2$ ($P < 0.0064$ for all cases). The pairwise $t$ test on the CEA-$\beta$ data adjusted by Bonferroni correction showed that the difference between the control and CEA was statistically significant when CEA was used at a concentration of 100 $\mu$M. The critical minimal concentrations at which significant differences were appearing for the data for CE-$\beta$, CE-$\beta_2$, and CEA-$\beta_2$ were $\geq$90, 30, and 30 $\mu$M, respectively.

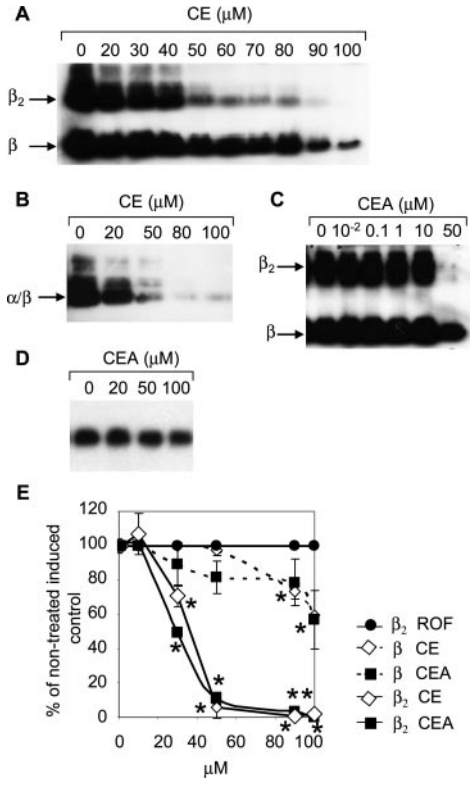


**Fig. 2.** Effect of CE and CEA on the secretion of the IL-12 forms from 3H10-HEK cells. A, 3H10-HEK cells were treated with CE for 24 h. Hexa-histidine-tagged $\beta$-chains were purified from the culture medium and subjected to a nonreducing 4 to 20% SDS-PAGE followed by immunodetection. B, immunodetection of the $\alpha\beta$ form in the growth medium of 3H10-HEK cells transfected with the $\alpha$-chain and treated with CE. C, 3H10-HEK cells were treated with CEA, and the $\beta$-chain was immunodetected as described in A. D, effect of CEA on the secretion of the housekeeping protein albumin after treatment of cells for 24 h and immunoblot. E, diagram plotting the levels of $\beta$, $\beta_2$ secretion after 24 h treatment with CE, CEA, or rofecoxib. Intensities of $\beta$ and $\beta_2$ from immunoblots were quantified by densitometric scanning. Values are expressed as means ± S.D. for five experiments. *, $P < 0.05$ for comparison with induced, nontreated control (pairwise $t$ test adjusted with Bonferroni correction).

Of the other NSAIDs we tested, neither ibuprofen nor indomethacin seemed to inhibit IL-12 secretion (Fig. 3). Inhibition of IL-12 secretion was observed for naproxen. However, because naproxen seemed to be pronouncedly cytotoxic when applied at concentrations $\geq$5 $\mu$M tested (Fig. 3), the decreased secretion of IL-12 is probably due to cell death and not to specific interference with the cellular IL-12 production pathway.

Finally, to ensure that the CE-/CEA-induced inhibition was not due to cytotoxic effects coinciding with decreased cell viability and ensuing hampered IL-12 secretion, we performed MTT tests on 3H10-HEK cells (Fig. 4). The $EC_{50}$ cytotoxicity values of CE and CEA were found to amount to 180 and 220 $\mu$M, respectively, thus ruling out generic cytotoxicity as a mechanistic cause for decreased IL-12 secretion.

**Effect of CE and CEA on Transcription of the $\alpha$- and $\beta$-Chains.** We used quantitative real-time RT-PCR to determine the effect of CE and CEA on transcription of $\alpha$- and $\beta$-chain genes. 3H10-HEK cells were cultured in the presence of increasing concentrations of CE or CEA for 2 h, followed by induction with ponasterone A. Twenty-two hours later, cells were collected, and total RNA was extracted and quantified. Subsequently, real-time RT-PCR was performed, and mRNA levels of the $\alpha$-chain, $\beta$-chain, and housekeeping gene (GADPH) were analyzed. Figure 5 shows that transcription of the $\beta$-chain was decreased with ~20% when cells were treated with 50 $\mu$M CE or CEA and that of the $\alpha$-chain with 25 to 40% at an identical concentration of CE or CEA, resulting in $IC_{50}$ values of >50 $\mu$M. The Kruskal-Wallis test was used to test for significant dose-response effects in the RT-PCR experiments (Fig. 5). The calculated $P$ values for the $\beta$-chain were 0.35 (CE) and 0.12 (CEA), and those for the $\alpha$-chain were 0.06 (CE) and 0.16 (CEA). Thus, the virtually complete inhibition of secretion into the culture medium of $\alpha\beta$ and $\beta_2$ at 50 $\mu$M CE or CEA (Fig. 2) cannot be explained by the assumption of a causative effect operating at the level of transcription.

**CE and CEA Modulate $Ca^{2+}$ Homeostasis in 3H10-HEK Cells.** The IL-12 $IC_{50}$ value of CE observed in this study coincides roughly with that of the COX2-independent effect of CE on the ER $Ca^{2+}$ ATPase (35 $\mu$M) reported by

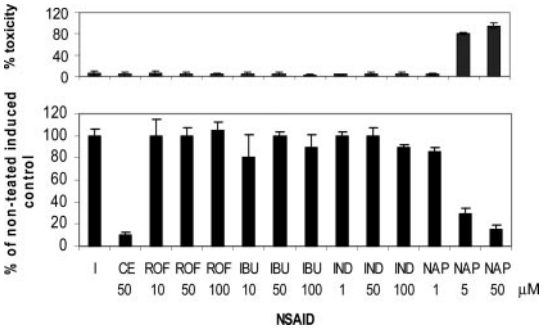


**Fig. 3.** Effect of NSAIDs on cell viability (top diagram) and $\beta_2$ homodimer secretion (bottom diagram). 3H10 cells were treated for 24 h with CE, rofecoxib (ROF), ibuprofen (IBU), indomethacin (IND), or naproxen (NAP). Nontreated induced cells were used as positive control (I) and CE-treated cells as negative control for $\beta_2$ secretion. Hexa-histidine-tagged $\beta$-chains were purified from the medium on $Ni^{2+}$-NTA agarose and eluates were submitted to nonreducing 4 to 20% SDS-PAGE and detected by immunoblot using the anti-$\beta$-chain antibody C8.6. Cytotoxicity of NSAIDs was measured after 24 h of treatment by means of the MTT assay. All bars represent the mean values over five experiments ± S.D.

Johnson et al. (2002). We verified whether CE and CEA affected the intracellular $Ca^{2+}$ levels in the cell line used in our experiments (i.e., 3H10-HEK cells). An increase of $[Ca^{2+}]_i$ was found to occur in cells treated with 50 $\mu$M CE or CEA, which was probably due to the depletion of intracellular calcium stores (Fig. 6A; Johnson et al., 2002). Rofecoxib used at a concentration of 50 $\mu$M did not exert any effect on calcium influx (Fig. 6A). Thus, hypothesizing that inhibition of IL-12 secretion by CE or CEA is related to the perturbation of $Ca^{2+}$ in the ER, we treated the 3H10-HEK cells with the known ER $Ca^{2+}$ ATPase inhibitor thapsigargin (TG) for 24 h. Indeed, thapsigargin completely blocked $\beta_2$ (Fig. 6B) and $\alpha\beta$ (data not shown) secretion at any of the concentrations tested, whereas similar to CE and CEA, it was less effective at inhibiting $\beta$ monomer secretion. Likewise, thapsigargin did not inhibit transcription of the $\alpha$- and $\beta$-chains at concentrations of 100 nM (data not shown).

**CEA Provokes Intracellular Retention and Increases Interaction of the $\beta_2$ Form of IL-12 with Calreticulin.** The results presented above suggest a possible relationship between CE-/CEA-mediated $Ca^{2+}$ perturbation and inhibition of IL-12 secretion. Secretory proteins normally have to be correctly folded in the ER before being authorized to exit the ER. The effect of $Ca^{2+}$ on ER protein folding is well documented (Corbett and Michalak, 2000). In further experiments, we focused on the effect of CE and CEA on the IL-12 folding pathway. We have identified previously glucose regulated protein-94, CRT, and protein disulfide isomerase as chaperones associating with the $\beta$-chain of IL-12 during transit in the ER (Alloza et al., 2004; Alloza and Vandenbroeck, 2005).

3H10-HEK cells were treated with CEA and were induced to produce IL-12 $\beta$ and $\beta_2$ with ponasterone A (Fig. 7A). After 16 h, cell media were collected, and cell lysates were prepared after cross-linking (or not) with DSP. IL-12 folding complexes were purified on an $Ni^{2+}$-NTA affinity chromatog-

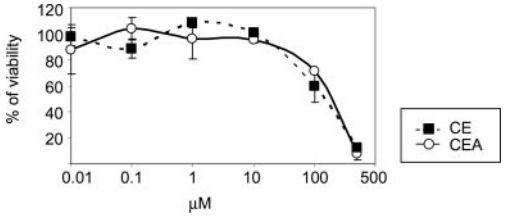


**Fig. 4.** Cytotoxicity of CE and CEA in 3H10-HEK cells. 3H10-HEK cells were seeded in 96-well plates and were treated with the concentrations of CE and CEA indicated during 24 h. After 2 h of incubation with MTT reagent, cells were dissolved in dimethyl sulfoxide. Optical density was measured in a spectrophotometer at 550 nm. The data represented are mean values ± S.D. from three experiments.

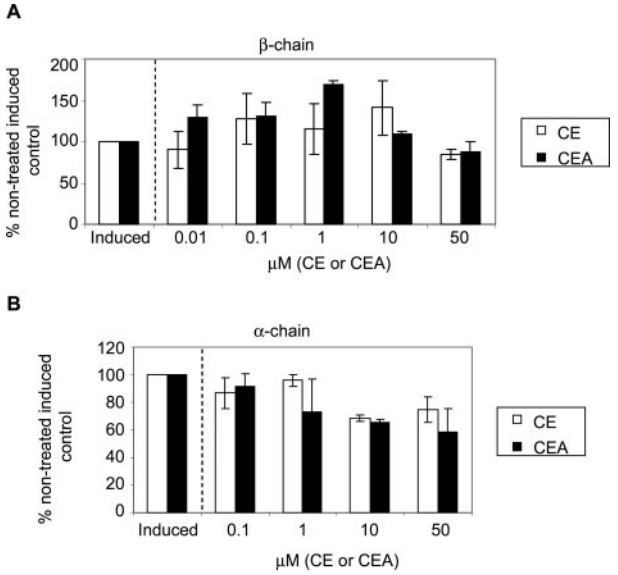


**Fig. 5.** Relative quantification of $\beta$- (A) and $\alpha$-chain (B) mRNA expression by real-time RT-PCR from 3H10-HEK cells treated with CE or CEA. After induction with ponasterone A, total RNA was extracted, and real-time RT-PCR was performed using the RT-PCR Quantitect Gene Expression Assay kit as explained under *Materials and Methods*. The mRNA levels of each gene were determined relative to GADPH housekeeper gene transcription. Values represent the percentages of picograms p35 or p40 per microgram of total RNA relative to induced, nontreated cells. The data represent the means ± S.D. from four experiments.

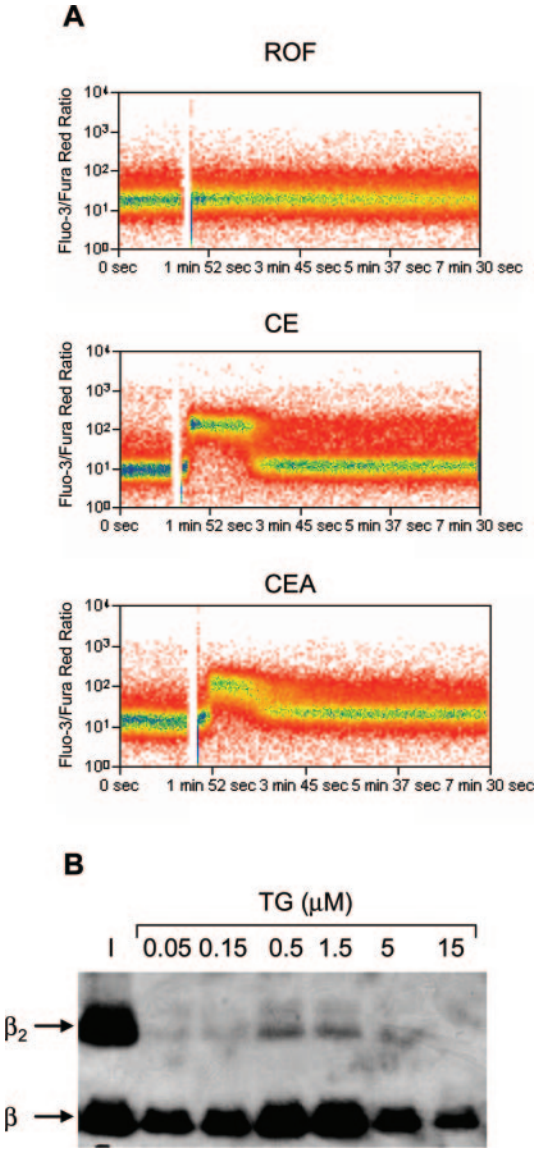


**Fig. 6.** A, Fluo-3/Fura-Red fluorescence ratio analysis of the effect of 50 $\mu$M CE, 50 $\mu$M CEA, and 50 $\mu$M ROF on $Ca^{2+}$ influx in 3H10-HEK cells. The fluorescence ratio versus time was analyzed by flow cytometry. B, 3H10-HEK cells were treated with increasing concentrations of TG followed by induction with ponasterone A during 24 h. The $\beta$ and $\beta_2$ forms were purified from the culture medium by means of $Ni^{2+}$-NTA chromatography, subjected to nonreducing 4 to 15% SDS-PAGE, and blotted. Detection was performed with the anti-$\beta$-chain antibody C8.6.

raphy, and eluates were submitted to SDS-PAGE. Figure 7A shows that, as expected, 50 $\mu$M CEA completely represses secretion of $\beta_2$. Analysis of intracellular fractions in Fig. 7B shows that in the presence of 50 $\mu$M CEA, both the $\beta$ and the $\beta_2$ forms are present intracellularly. Thus, the lack of secretion of $\beta_2$ at this concentration of CEA does not seem to result from an impediment in the $\beta$-chain dimerization reaction but rather from intracellular retention of the dimer form. In the presence of CEA, the $\beta$-chain of IL-12 showed a strongly increased interaction with the $Ca^{2+}$-dependent chaperone CRT (Fig. 7, C and D), and under these conditions, approximately five times more calreticulin was coimmunoprecipitated with the His-tagged $\beta$-chain than in induced, untreated cells. The Kruskal-Wallis test was used to test for significant differences in relative amounts of cocaptured CRT with $\beta$-chain compared with control (Fig. 7). This revealed a significant difference between the treatment groups and was therefore followed by pairwise $t$ tests adjusted by the Bonferroni correction. The result showed no significant difference for all pairwise comparisons between 25 $\mu$M CEA (+DSP), 50 $\mu$M CEA (−DSP), and 50 $\mu$M CEA (+DSP) ($P > 0.35$). Pairwise comparison between uninduced and induced control cells was also not significant ($P = 0.93$). However, all pairwise comparisons between any of 25 $\mu$M CEA (+DSP), 50 $\mu$M CEA (−DSP), or 50 $\mu$M (+DSP) on the one hand and induced or uninduced controls on the other hand showed significant differences ($P \leq 0.03$). The interaction between CRT and IL-12 was seen both in the presence or absence of the homobifunctional cross-linker DSP (Fig. 7C, compare lanes 6 and 8).

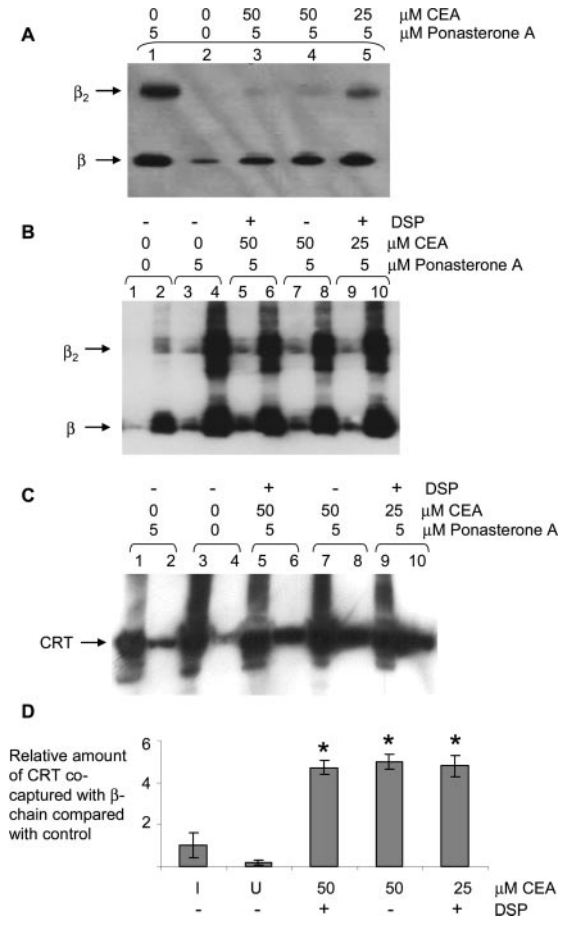


**Fig. 7.** A, CEA inhibits secretion of the $\beta_2$ homodimer. 3H10-HEK cells were induced with ponasterone A (lanes 1 and 3–5) or not (lane 2) and treated with the concentrations of CEA indicated. Culture medium was collected after 16 h of induction and submitted to nonreducing 4 to 20% SDS-PAGE and anti-$\beta$-chain C8.6 immunoblot. B, CEA does not inhibit intracellular formation of the IL-12 $\beta_2$ form. Intracellular $\beta$-chain was purified from these cells by means of $Ni^{2+}$-NTA agarose in the presence of NEM to alkylate free sulfhydryl groups. Before cell lysis, cells were incubated with the cross-linker DSP or not (as indicated). Flow-through (lanes 1, 3, 5, 7, and 9) and eluted (lanes 2, 4, 6, 8, and 10) fractions were mixed with equal volumes of 2× nonreducing loading solution and submitted to 10% nonreducing SDS-PAGE. Western blot detection was carried out using anti-$\beta$-chain antibody C8.6. C, CEA increases the interaction between CRT and the $\beta$-chain. Fractions of the cell lysates before purification (lanes 1, 3, 5, 7, and 9) and of the $Ni^{2+}$-NTA-eluted fractions (lanes 2, 4, 6, 8, and 10) were mixed with 2× reducing SDS-PAGE loading solution, boiled at 95°C for 5 min, and submitted to 10% reducing SDS-PAGE. Western blot detection was carried out using anticalreticulin antibody (SPA-600). D, intensities of CRT bands were quantified by densitometric scanning from the immunoblots. U, uninduced control cells; I, induced nontreated control cells; ASU, arbitrary scanning units. *, $P < 0.03$ for comparison with I or U (pairwise $t$ test adjusted with Bonferroni correction).

**CEA Inhibits Interaction Between IL-12 and ERp44.** ERp44 is a recently identified chaperone that is crucial in thiol-mediated retention of oxidative folding and assembly intermediates of oligomeric proteins (Anelli et al., 2003). To investigate a putative role of this chaperone in inhibition of IL-12 secretion by CEA, 3H10-HEK cells were transfected with HA-ERp44 wt, HA-ERp44 C29S, or HA-ERp44 ΔRDEL (Anelli et al., 2002). HA-ERp44 copurified with IL-12 on an $Ni^{2+}$-NTA affinity chromatography was detected in immunoblot with anti-HA monoclonal antibody. In untreated cells, IL-12 interacted with wild-type ERp44 (Fig. 8A). This interaction was decreased in cells transfected with the ERp44 C29S and ΔRDEL mutants. This is in accordance with the notion of cysteine 29 of ERp44 being involved in complex formation with IL-12, as shown previously for other cargo proteins (Anelli et al., 2003). ERp44 lacking the ER retention motif RDEL is secreted and was therefore, as expected, less

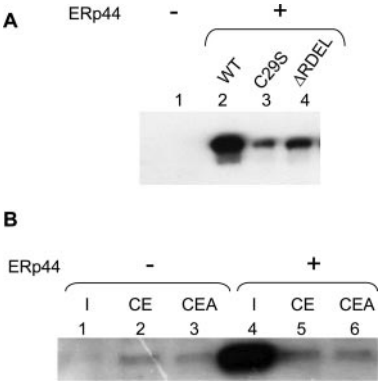


**Fig. 8.** A, association of ERp44 with IL-12. 3H10-HEK cells were transfected with HA-tagged ERp44 (wt, C29S, or ΔRDEL). After 24 h, cells were induced with ponasterone A and incubated for a further 24 h. Cells were washed and lysed followed by immunoprecipitation on a $Ni^{2+}$-NTA affinity chromatography columns as indicated under *Materials and Methods*. Copurified HA-tagged ERp44 was detected using the mouse monoclonal HA-antibody (12CA5). Lane 1, untransfected 3H10-HEK cells; lane 2, 3H10-HEK cells transfected with HA-tagged ERp44 wt; lane 3, 3H10-HEK cells transfected with HA-tagged ERp44 C29S; and lane 4, 3H10-HEK cells transfected with HA-tagged ERp44 ΔRDEL. B, CE and CEA decrease the interaction between IL-12 and ERp44. 3H10-HEK cells were transfected or not with HA-tagged ERp44 wt. 3H10-HEK cells were induced for 24 h with ponasterone A, treated (lanes 2, 3, 5, and 6) or not (lanes 1 and 4) with CE or CEA, followed by immunoprecipitation and detection as described in A.

efficiently recruited to the IL-12 folding complex. When cells were treated with 50 μM CE or CEA, the wild-type ERp44 was found not to interact with IL-12 (Fig. 8B). Thus, both the increased interaction of IL-12 with the "quality control" chaperone CRT and the decreased interaction with Erp44 indicate that altered chaperone usage and folding of IL-12 in the ER may constitute a plausible mechanism underlying the inhibitory effects of CE or CEA on IL-12 secretion.

**Kinetics of α, β, αβ, and $\beta_2$ Secretion.** In the 3H10 HEK cells used in this study the α- and β-chains are transcribed from identical ponasterone A-inducible promoters [pIND(SP1)]. Furthermore, we designed the expression cassettes to ensure that 1) translation of both chains is initiated from identical Kozak sequences (Alloza et al., 2004) and 2) the authentic 3′-untranslated regions and polyadenylation sites of the α- and β-chains were replaced with those of bovine growth hormone. This guaranteed that kinetics of transcription and translation would be similar for both the α- and β-chains. Any differences in the time it takes for monomeric and dimeric IL-12 chains to appear in the medium after induction should therefore be correlated to the time needed to complete intracellular transit and, hence, to differences in post-translational stages of protein processing, chaperone interaction, and folding. Figure 9 shows that immunodetectable β-monomer appeared in the medium with a $t_{1/2}$ of ~2 h, whereas $\beta_2$ was secreted with a $t_{1/2}$ of ~7 h. The relative kinetics for secretion were $\beta \gg \alpha\beta > \beta_2$. The much slower kinetics of $\beta_2$ compared with β secretion invokes complex reactions involving β homodimer assembly and, taken together with the above data on chaperone usage, suggests that the β monomer is less sensitive to the inhibitory effect of CE/CEA on secretion as a result of its folding occurring (largely) spontaneously (i.e., probably independent from the action of $Ca^{2+}$-dependent chaperones and accessory factors).

## Discussion

In this study, we have shown that both celecoxib and an analog devoid of COX2-inhibitory activity potently block the secretion of the αβ and $\beta_2$ dimeric forms of IL-12 and, when applied at higher concentration, that of the β monomer (Fig. 2, A and B). Further experiments showed that that these effects were not due to the inhibition of transcription of the α- or β-chain (Fig. 5). Evidence that the mechanism used by CE to interfere with folding and secretion of IL-12 is independent from COX2 inhibition arises from the following facts. First, other NSAIDs, including ibuprofen, indomethacin, and the selective COX2 inhibitor rofecoxib, were found not to have any effect on secretion of IL-12 (Fig. 3; naproxen seemed to be cytotoxic in our assay). Indeed, it has been described previously that celecoxib can display COX2-independent modes of action that are not seen with other COX2 inhibitors (i.e., rofecoxib) (Fig. 10). Patel et al. (2005), for instance, have shown that whereas CE provokes inhibition of cell growth in prostate cancer, rofecoxib has no such effect. Second, CEA, an analog of CE lacking the COX2 inhibition, shows effects identical with those of CE on folding/secretion of IL-12. Others have also used inactive COX2 derivatives of CE to prove a COX2-independent mechanism of CE (Kulp et al., 2004). Third, the $IC_{50}$ value at which we observe inhibition of IL-12 coincides roughly with the $IC_{50}$ values reported in the literature for most COX2-independent mechanisms of CE (Fig. 10; Tegeder et al., 2001).

Previous studies have reported that at low concentrations, CE increases IL-12 transcription in a COX2-dependent manner (Stolina et al., 2000; Vandenbroeck et al., 2004). This is not in discrepancy with our findings in view of the fact that the concentrations used by Stolina et al. (2000) did not reach the $IC_{50}$ values reported for any of the COX2-independent

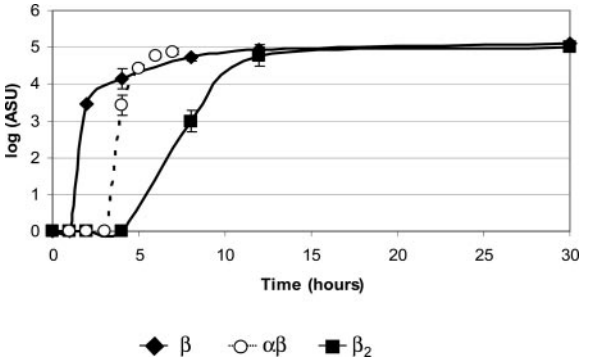


**Fig. 9.** Kinetics of secretion of β, αβ, and $\beta_2$ forms of IL-12 from 3H10-HEK cells (β and $\beta_2$) and 3H10-HEK cells transiently transfected with pIND(SP1)-p35 (αβ). Secreted IL-12 forms were quantified by densitometric scanning from immunoblots. The data represent the means ± S.D. from three experiments. ASU, arbitrary scanning units.

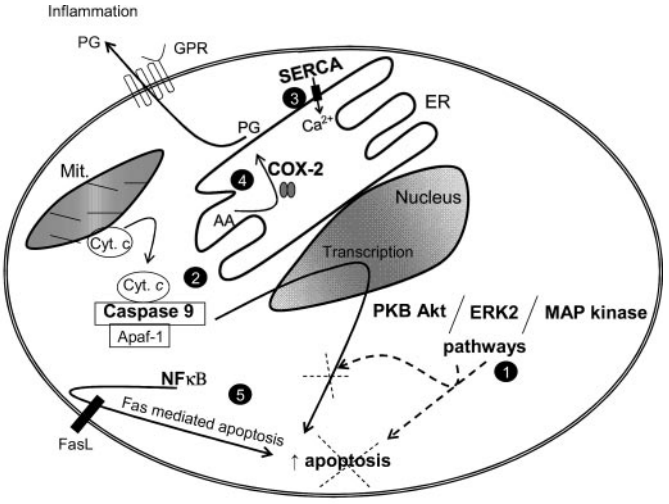


Celecoxib effects

1. Negative regulation of PKB Akt /ERK2/MAP, $IC_{50}$≥ 50 μM (Hsu et al., 2000; Sun and Sinicropel, 2005; Takahashi et al., 2005)
2. Positive regulation of caspase 9, $EC_{50}$=75 μM (Ding et al., 2005)
3. Negative regulation of SERCA, $IC_{50}$=35 μM (Johnson et al., 2002; Wang et al., 2004; Tanaka et al., 2005)
4. Negative regulation of COX-2, $IC_{50}$=0.04 μM (DeWitt 1999)
5. Positive regulation of NFκB, 50 μM (Niederberger et al., 2001)

**Fig. 10.** Important celecoxib effects. ❶, the components represented are involved in cell survival signaling pathways, and they also inhibit caspase-9-induced apoptosis (see broken lines). Celecoxib has been shown to cause apoptosis by negatively regulating protein kinase B Akt/extracellular signal-regulated kinase-2/mitogen activated protein kinase pathways (PKB Akt/ERK2/MAP). ❷, the cytochrome *c* released from the mitochondria activates caspase 9, which in turn induces apoptosis. Celecoxib is known to induce this activation. ❸, sarco(endo)plasmic reticulum $Ca^{2+}$ ATPase (SERCA) or ER-$Ca^{2+}$ ATPase are involved in the uptake of calcium into the ER. It has been demonstrated that celecoxib inhibits this uptake. ❹, COX2 is involved in the conversion of arachidonic acid into prostaglandins. Celecoxib was originally described as a COX2 inhibitor. ❺, nuclear factor κB (NF-κB) plays a role in Fas-mediated apoptosis. Celecoxib is known to positively regulate this pathway.

mechanisms, including the effect on folding/secretion of IL-12 reported in this article. Thus, at a micromolar concentration range, CE is likely to "over-ride" its transcription-dependent stimulatory effect on IL-12 production by blocking COX2-independent transit of the protein in the ER.

We undertook to determine by which mechanism(s) celecoxib inhibits the production of $\alpha\beta$ and $\beta_2$ forms of IL-12. Given the lack of effect of CE and CEA on transcription, the absence of secretion of the $\beta_2$ and $\alpha\beta$ forms could theoretically be due either to an impediment in the assembly of the dimer forms or to selective intracellular retention of the dimer, but not monomer, forms. However, whichever mechanism applies, it is likely to take place in the secretory pathways of the ER and/or Golgi apparatus, in which folding and maturation of secretory proteins occur (Ellgaard et al., 1999). Of all studies published on non-COX2-related effects of CE, the article by Johnson et al. (2002) may be of particular relevance because it provides evidence for a $Ca^{2+}$ perturbance in the ER, with an $EC_{50}$ value similar to that observed for inhibition of IL-12 in this study (i.e., 50 $\mu$M). CE and CEA were found to modulate intracellular $Ca^{2+}$ levels in 3H10-HEK cells in this study (Fig. 6). The role of $Ca^{2+}$ in protein folding and chaperone usage in the ER is well documented (Corbett and Michalak, 2000). Further indications for a role of $Ca^{2+}$ in IL-12 folding come from the use of TG, a known ER-$Ca^{2+}$ ATPase inhibitor, which we found to potently block the secretion of dimeric forms of IL-12 and, to a lesser extent, that of the $\beta$ monomer (Fig. 6). TG has been shown as well to inhibit the secretion of other multisubunit proteins including thyroglobulin (TH). TH is a homodimer that follows a complex folding procedure (Di Jeso et al., 2003); depletion of calcium in the endoplasmic reticulum causes stabilization of interaction of chaperones with TH. Retention of incompletely or incorrectly folded secretory proteins normally occurs at the level of ER. Such proteins cannot bypass the ER "quality control" system and are retained in the ER and/or degraded (Kopito, 1997). In the presence of CE, calreticulin, a known folding quality control factor in the ER, is strongly associated with IL-12. In normal conditions, CRT assists the folding of IL-12 (Alloza et al., 2004). ER $Ca^{2+}$ depletion may inhibit the release of CRT from IL-12. On the other hand, IL-12 may fail to dimerize properly because of the lower activity of some chaperones caused by the depletion of $Ca^{2+}$ in the ER (Corbett and Michalak, 2000) and is therefore intercepted by CRT.

Further evidence for a pronounced effect of CE on IL-12 folding followed from ERp44 cotransfection experiments. The novel chaperone ERp44 is involved in the oxidative folding pathway of many oligomeric proteins and operates through thiol-mediated retention of oxidative folding and assembly intermediates (Anelli et al., 2002). The cysteine residue at position 29 in ERp44 is used to form covalent disulfide bonds with cargo proteins such as Ero1$\alpha$ and immunoglobulins (Anelli et al., 2003). Given the dependence of correct IL-12 dimerization on establishment of suitable disulfide bonds, it is reasonable to consider this cytokine as a client protein of ERp44. ERp44 was found to interact with IL-12 in untreated cells but was not able to associate with IL-12 when cells had been treated with CE or CEA, an effect probably related to IL-12 misfolding induced by CE/CEA (Fig. 9).

The in vitro effects we have reported occur at concentrations well above those needed to inhibit COX2. It will therefore be important to address the potential pharmacological significance in vivo. Davies et al. (2000) have reported a peak human plasma concentration of celecoxib after oral administration of up to 8 $\mu$M, whereas others have reported celecoxib serum concentrations from 20 to 100 $\mu$M (Basu et al., 2005). No literature data are available on tissue or cell concentrations of celecoxib in vivo, making it difficult to correlate in vitro effects with potential pharmacological effects in vivo. The in vitro effects on IL-12 folding and secretion reported here take place at a concentration of celecoxib ($IC_{50}$ of 20–30 $\mu$M) that seems to be achievable in human plasma upon oral administration and that therefore may directly affect the mobile plasma cells (i.e., macrophages and dendritic cells), which constitute the natural producer cell source of IL-12 (Brombacher et al., 2003). These effects might be more pronounced in individuals with reduced clearance or metabolization of celecoxib (i.e., individuals with reduced hepatic function or specific genetic constitution). Indeed, the steady-state area under the plasma concentration-time curve of celecoxib is increased up to 180% in patients with moderate hepatic impairment (Davies et al., 2000). Celecoxib is metabolized principally by the cytochrome P450 2C9 isoenzyme. Tang et al. (2001) reported that based on a simulation of in vitro data, *CYP2C9* genotype may increase the celecoxib plasma area under the plasma concentration-time curve by up to 500% (Tang et al., 2001).

In summary, we have demonstrated that CE and CEA block the production of IL-12 by a mechanism that is independent of COX2 inhibition. We have demonstrated that ERp44 and CRT are ER factors that may be involved in the blockage of IL-12 production when cells are treated with CE and CEA. Our data indicate that targeting the ER to impede the production of IL-12 may be considered as a novel approach to block cytokine production. CE-mediated alterations in the secretome should be investigated as a contributing factor to some of the adverse effects of this drug.

**Acknowledgments**

We thank Roberto Sitia and Tiziana Anelli (San Raffaele Scientific Institute, Milan, Italy) for kindly providing us with the ERp44 constructs and detection reagents.

**References**

Alloza I, Martens E, Hawthorne S, and Vandenbroeck K (2004) Cross-linking approach to affinity capture of protein complexes from chaotrope-solubilized cell lysates. *Ann Biochem* **324:**137–142.

Alloza I and Vandenbroeck K (2005) The metallopeptide antibiotic bacitracin inhibits interleukin-12 $\alpha\beta$ and $\beta_2$ secretion. *J Pharm Pharmacol* **57:**213–218.

Anelli T, Alessio M, Bachi A, Bergamelli L, Bertoli G, Camerini S, Mezghrani A, Ruffato E, Simmen T, and Sitia R (2003) Thiol-mediated protein retention in the endoplasmic reticulum: the role of ERrp44. *EMBO (Eur Mol Biol Organ) J* **22:** 5015–5022.

Anelli T, Alessio M, Mezghrani A, Simmen T, Talamo F, Bachi A, and Sitia R (2002) ERp44, a novel endoplasmic reticulum folding assistant of the thioredoxin family. *EMBO (Eur Mol Biol Organ) J* **21:**835–844.

Basu GD, Pathangey LB, Tinder TL, Gendler SJ, and Mukherjee P (2005) Mechanisms underlying the growth inhibitory effects of the cyclo-oxygenase-2 inhibitor celecoxib in human breast cancer cells. *Breast Cancer Res* **7:**R422–R435.

Brombacher F, Kastelein RA, and Alber G (2003) Novel IL-12 family members shed light on the orchestration of Th1 responses. *Trends Immunol* **24:**207–212.

Corbett EF and Michalak M (2000) Calcium, a signaling molecule in the endoplasmic reticulum? *Trends Biochem Sci* **25:**307–311.

Davies NM, McLachan AJ, Day RO, and Williams KM (2000) Clinical pharmacokinetics and pharmacodynamics of celecoxib: a selective cyclo-oxygenase-2 inhibitor. *Clin Pharmacokinet* **38:**225–242.

DeWitt DL (1999) Cox-2-selective inhibitors: the new super aspirins. *Mol Pharmacol* **55:**625–631.

Di Jeso B, Ulianich L, Pacifico F, Leonardi A, Vito P, Consiglio E, Formisano S, and Arvan P (2003) Folding of thyroglobulin in the calnexin/calreticulin pathway and its alteration by loss of $Ca^{2+}$ from the endoplasmic reticulum. *Biochem J* **370:**449–458.

Ding HM, Han CH, Zhu JX, Chen CS, and D'Ambrosio SM (2005) Celecoxib derivatives induce apoptosis via the disruption of mitochondrial membrane potential and activation of caspase 9. *Int J Cancer* **113:**803–810.
Ellgaard L, Molinari M, and Helenius A (1999) Setting the standards: quality control in the secretory pathway. *Science (Wash DC)* **286:**1882–1888.
Grosch S, Tegeder I, Niederberger E, Brautigam L, and Geisslinger G (2001) COX-2 independent induction of cell cycle arrest and apoptosis in colon cancer cells by the selective COX-2 inhibitor celecoxib. *FASEB J* **15:**2742–2744.
Ha SF, Lee CH, Lee SB, Kim CM, Jang KL, Shin HS, and Sung YC (1999) A novel function of Il-12p40 as chemotactic molecule for macrophages. *J Immunol* **163:** 2902–2908.
Hsu AL, Ching TT, Wang DS, Song XQ, Rangnekar VM, and Chen CS (2000) The cyclooxygenase-2 inhibitor celecoxib induces apoptosis by blocking Akt activation in human prostate cancer cells independently of Bcl-2. *J Biol Chem* **275:**11397–11403.
Johnson AJ, Hsu AL, Lin HP, Song XQ, and Chen CS (2002) The cyclo-oxigenase-2 inhibitor celecoxib perturbs intracellular calcium by inhibiting endoplasmic reticulum $Ca^{2+}$-ATPases: a plausible link with its anti-tumor effect and cardiovascular risks. *Biochem J* **366:**831–837.
Kopito RR (1997) ER quality control: the cytoplasmic connection. *Cell* **88:**427–430.
Kulp SK, Yang YT, Hung CC, Chen KF, Lai JP, Tseng PH, Fowble JW, Ward PJ, and Chen CS (2004) 3-Phosphoinositide-dependent protein kinase-1/Akt signaling represents a major cyclooxygenase-2-independent target for celecoxib in prostate cancer cells. *Cancer Res* **64:**1444–1451.
Niederberger E, Tegeder I, Vetter G, Schimdtko A, Schmidt H, Euchenhofer C, Bräutigam L, Grösch S, and Geisslinger G (2001) Celecoxib loses its anti-inflammatory efficacy at high doses by activation of NF-$\kappa\beta$. *FASEB J* **15:**1622–1624.
Patel MI, Subbaramaiah K, Du BH, Chang M, Yang PY, Newman RA, Cordon-Cardo C, Thaler HT, and Dannenberg AJ (2005) Celecoxib inhibits prostate cancer growth: evidence of a cyclooxygenase-2-independent mechanism. *Clin Cancer Res* **11:**1999–2007.
Penning TD, Talley JJ, Bertenshaw SR, Carter JS, Collins PW, Docter S, Graneto MJ, Lee LF, Malecha JW, Miyashiro JM, et al. (1997) Synthesis an biological evaluation of the 1,5-diarylpyrazole class of cyclooxygenase-2 inhibitors: identification of 4-[5-(4-methylphenyl)-3-(trifluoromethyl)-1*H*-pyrazol-1-yl]benzenesulfonamide (SC-58635, celecoxib) *J Med Chem* **40:**1347–1365.
Prescott SM and Fitzpatrick FA (2000) Cyclooxygenase-2 and carcinogenesis. *Biochim Biophys Acta* **1470:**M69–M78.
Saini SS, Gessell-Lee DL, and Peterson JW (2003) The cox-2-specific inhibitor celecoxib inhibits adenyl cyclase. *Inflammation* **27:**79–88.
Sheng HM, Shao JY, Kirkland SC, Isakson P, Coffey RJ, Morrow J, Beauchamp RD, and DuBois RN (1997) Inhibition of human colon cancer cell growth by selective inhibition of cyclooxygenase-2. *J Clin Investig* **99:**2254–2259.
Stolina M, Sharma S, Lin Y, Dohadwala M, Gardner B, Luo J, Zhu L, Kronenberg M, Miller PW, Portanova J, et al. (2000) Specific inhibition of cyclooxygenase 2 restores antitumor reactivity by altering the balance of IL-10 and IL-12 synthesis. *J Immunol* **164:**361–370.
Subbaramaiah K, Telang N, Ramonetti JT, Araki R, DeVito B, Weksler BB, and Dannenberg AJ (1996) Transcription of cyclooxygenase-2 is enhanced in transformed mammary epithelial cells. *Cancer Res* **56:**4424–4429.
Sun YJ and Sinicropel FA (2005) Selective inhibitors of MEK1/ERK44/42 and p38 mitogen-activated protein kinases potentiate apoptosis induction by sulindac sulfide in human colon carcinoma cells. *Mol Cancer Ther* **4:**51–59.
Takahashi T, Ogawa Y, Kitaoka K, Tani T, Uemura Y, Taguchi H, Kobayashi T, Seguchi H, Yamamoto A, and Yoshida S (2005) Selective COX-2 inhibitor regulates the MAP kinase signaling pathway in human osteoarthritic chondrocytes after induction of nitric oxide. *Int J Mol Med* **15:**213–219.
Tanaka K, Tomisato W, Hoshino T, Ishihara T, Namba T, Aburaya M, Katsu T, Suzuki K, Tsutsumi S, and Mizushima T (2005) Involvement of intracellular $Ca^{2+}$ levels in nonsteroidal anti-inflammatory drug-induced apoptosis. *J Biol Chem* **280:**31059–31067.
Tang C, Shou M, Rushmore TH, Mei Q, Sandhu P, Woolf EJ, Rose MJ, Gelmann A, Greenberg HE, De Lepeleire I, et al. (2001) In vitro metabolism of celecoxib, a cyclooxygenase-2 inhibitor, by allelic variant forms of human liver microsomal cytochrome P450 2C9: correlation with CYP2C9 genotype and in vivo pharmacokinetics. *Pharmacogenetics* **11:**223–235.
Tegeder I, Pfeilschifter J, and Geisslinger G (2001) Cyclooxygenase-independent actions of cyclooxygenase inhibitors. *FASEB J* **15:**2057–2072.
Trembleau S, Germann T, Gately MK, and Adorini L (1995) The role of IL-12 in the induction of organ-specific autoimmune-diseases. *Immunol Today* **16:**363–386.
Vandenbroeck K, Alloza I, Gadina M, and Matthys P (2004) Inhibiting cytokines of the interleukin-12 family: recent advances and novel challenges. *J Pharm Pharmacol* **56:**145–160.
Vane JR, Mitchell JA, Appleton I, Tomlinson A, Bishopbailey D, Croxtall J, and Willoughby DA (1994) Inducible isoforms of cyclooxygenase and nitric-oxide synthase in inflammation. *Proc Natl Acad Sci USA* **91:**2046–2050.
Vivanco I and Sawyers CL (2002) The phosphatidylinositol 3-kinase-AKT pathway in human cancer. *Nat Rev Cancer* **2:**489–501.
Walter MJ, Kajiwara N, Karanja P, Castro M, and Holtzman MJ (2001) Interleukin-12 p40 production by barrier epithelial cells during airway inflammation. *J Exp Med* **193:**339–351.
Wang JL, Lin KL, Chen JS, Lu YC, Jiann BP, Chang HT, Hsu SS, Chen WC, Huang JK, Ho CM, et al. (2004) Effect of celecoxib on $Ca^{2+}$ movement and cell proliferation in human osteoblasts. *Biochem Pharmacol* **67:**1123–1130.
Waskewich C, Blumenthal RD, Li HL, Stein R, Goldenberg DM, and Burton J (2002) Celecoxib exhibits the greatest potency amongst cyclooxygenase (COX) inhibitors for growth inhibition of COX-2-negative hematopoietic and epithelial cell lines. *Cancer Res* **62:**2029–2033.
Zar JH (1999) Multisample hypotheses: the analysis of variance, in *Biostatistical Analysis*, 4th ed, pp 177–206, Prentice-Hall, Inc., Upper Saddle River, NJ.

**Address correspondence to:** Dr. Koen Vandenbroeck, Chair in Applied Genomics, School of Pharmacy, Queen's University Belfast, 97 Lisburn Road, Belfast BT3 7BL, UK. E-mail: k.vandenbroeck@qub.ac.uk